Morphology Development and Interfacial Erosion in Reactive Polymer Blending

Prashant A. Bhadane,[†] Andy H. Tsou,[‡] John Cheng,[§] and Basil D. Favis*[,†]

CREPEC, Department of Chemical Engineering, École Polytechnique de Montréal, 2900 Édouard Montpetit, P.O. Box 6079, Station Centre-Ville, Montréal, Québec, Canada H3C 3A7; Corporate Strategic Research, ExxonMobil Research and Engineering Company, 1545 Route 22 East, Annandale, New Jersey 08801; and Global Specialty Polymers Technology, ExxonMobil Chemical Company, 5200 Bayway Dr., Baytown, Texas 77520

Received June 20, 2008; Revised Manuscript Received August 4, 2008

ABSTRACT: This work studies morphology development in blends of polyamide (PA) with poly(isobutylene-*co*-*p*-methylstyrene) (IMSM) and brominated poly(isobutylene-*co*-*p*-methylstyrene) (BIMSM). The presence of pendent benzylic bromine in BIMSM facilitates the rapid in situ formation of BIMSM−PA graft copolymer. IMSM represents the nonreactive reference for this blend system. In this study several important anomalies have been observed for the reactive BIMSM/PA system as compared to classical interfacially modified blend systems. These anomalies are as follows: as much as a 37-fold reduction in volume average diameter for the reactive system as compared to the nonreactive one; high phase size distribution (d_v/d_n), at all blend compositions, with the fine droplets being in the 50−80 nm range scale; extensive droplet in droplet formation for BIMSM in PA in a BIMSM matrix; very high extents of reaction, i.e., 46 wt % of the total blend material reacts over a short time of mixing; and an emulsification study which demonstrates a linear drop in particle size and requires a very high concentration of copolymer (20 IMSM/80 BIMSM) to reach a plateau value. This is well beyond the amount of copolymer needed to saturate the interface even though static interfacial tension studies show that only 5% BIMSM in IMSM completely suppresses capillary breakup. These results are explained by a novel mechanism of reactive morphology development termed here as "interfacial erosion". The mechanism considers the formation of a very high viscosity graft copolymer right at the interface during dynamic mixing, resulting from the mutual contact of the BIMSM and PA molecules. The viscosity mismatch between the formed graft copolymer and the other constituents of the blend lead to the subsequent erosion of interphase material during dynamic mixing to form fine, nanometer-sized micelles in the bulk. The removal of the copolymer from the interface exposes nonreacted material and primes the interfacial region for further copolymer formation. In this fashion, most of the BIMSM can be made to react, and the resulting blend is a nanoscale dispersion with a number-average diameter of 50−80 nm and a volume average diameter of 300 nm. This work raises important considerations concerning the use of graft copolymers, in general, in polymer blend systems.

Introduction

The modification of interfaces in heterophase polymer blend systems and its subsequent influence on the phase morphology are crucial toward obtaining novel materials with improved physical properties.[1−5] Much of the work related to this topic in the scientific literature has focused on the addition of premade diblock, triblock, and even random-type copolymers.[6−9] Considerably less work has been published on the efficacy of graft polymers despite the fact that the in situ generation of graft copolymers between two mutually reactive species constitutes the principal protocol used in industrial practice. In the classical sense, efficacy generally refers to the effectiveness of the copolymer to situate itself at the interface and reduce the interfacial tension and particle−particle coalescence.

The modification of the interface influences the phase morphology principally through the reduction in interfacial tension and coalescence suppression.[8−12] Several studies have examined the effect of copolymer concentration on interfacial tension. *Without exception,* an initial rapid drop in interfacial tension is observed at very low copolymer concentrations followed by a plateau behavior at somewhat higher copolymer concentrations. Since the evolution of dispersed phase particle size as a function of copolymer (an emulsification study) is dominated by changes in the interfacial tension and particle−particle coalescence, an analogous behavior to that of interfacial tension is observed, i.e., a rapid drop in phase size followed by a plateau value.[7,8,12−15] This is true even for classical emulsions. Typically, the phase size reduction ranges between 2- and 7-fold, and the critical copolymer concentration required to obtain the plateau value ranges between 0.5 and 20 wt % based on the minor phase. This critical concentration has been related to the saturation of the interface by interfacial modifier, and beyond that concentration, micelles of copolymer (typically nanometer sized) are generated in the bulk phases.

Fundamentally, parameters such as the copolymer molecular weight, chemical composition, and architecture have been found to be critical with respect to the efficacy of the copolymer in blend emulsification.[7,8,16−19] Several authors have studied the influence of these parameters, both theoretically and experimentally. Higher molecular weight copolymers can occupy more area per molecule at the interface, and therefore, typically, the critical concentration for interfacial saturation decreases with an increase in copolymer molecular weight. However, it has been reported that the copolymer molecular weight has little influence on the plateau value phase size.[7,8] An increase in the copolymer molecular weight also increases the tendency of copolymer micelle formation.[6−8,17,19]

The composition of the copolymer plays an important role in its emulsification efficacy. Generally, symmetric copolymers are more effective at reducing the interfacial tension and drive

* Corresponding author: e-mail basil.favis@polymtl.ca; Tel +1-514-340-4711, ext 4527; Fax +1-514-340-4159.
[†] École Polytechnique de Montréal.
[‡] ExxonMobil Research and Engineering Company.
[§] ExxonMobil Chemical Company.

10.1021/ma801390s CCC: $40.75
Published on Web 09/23/2008

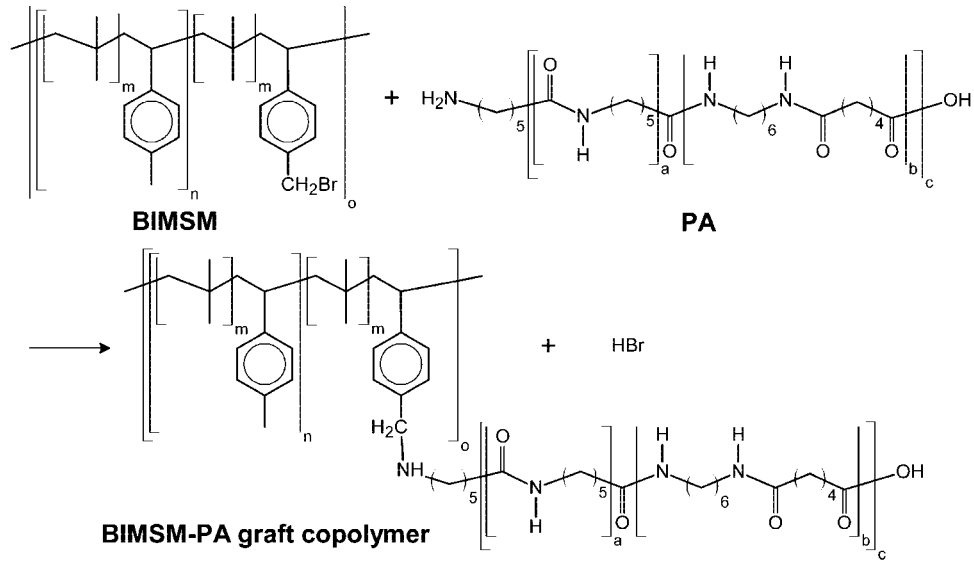

Figure 1. Reaction between BIMSM and PA to form a BIMSM−PA graft copolymer.

very effectively to the interface.[7,8,16,20] Asymmetric copolymers demonstrate an increased tendency for micelle formation and tend to form micelles in the same phase for which it is composition-rich.[8,12,16,18]

The copolymer architecture is one of the most important parameters affecting its capacity to emulsify. Comprehensive experimental and theoretical treatments are available on diblock, triblock, and random-block copolymer architectures,[6−8,16,20] but not much information, especially experimental data, is available on comb-type copolymer architectures. Theoretically using analytical arguments and numerical self-consistent field calculations, Lyatskaya et al.[20,21] compared the effectiveness of diblock, star, and comb-type copolymers. Comb-type copolymers were found to be more effective at reducing the interfacial tension than diblocks.[20−24] Their efficacy is a function of the molecular weight and length of backbone and teeth, the number of teeth, and the spacing between two adjacent teeth. The higher molecular weight combs and number of teeth corresponding to a symmetric comb composition were found to be the most effective at reducing interfacial tension.[20−24] Experimentally, Yilgor et al.[24] found comb copolymers were indeed more effective at reducing interfacial tension than regular diblocks. Peiffer et al.[4] found the grafts significantly enhance tensile properties. The improvement is directly related to the number of grafts per chain and its molecular weight.

Compared to premade copolymers, which must diffuse to the interface, graft copolymers formed in situ right at the interface are more effective at reducing interfacial tension. Some common reactions during reactive compatibilization include amine/anhydride, carboxylic acid/epoxy, amine/epoxy, and isocyanate/amine, as well as others. Polyamide-based reactively compatibilized systems constitute a major portion of reactive compatibilization studies.[1,25−27]

Brominated poly(isobutylene-*co*-*p*-methylstyrene) (BIMSM) is a novel elastomer. It is a random copolymer of isobutylene (IB), *p*-methylstyrene (PMS), and brominated PMS. This elastomer carries many pendent bromine moieties along its saturated backbone which can be utilized for in situ graft copolymer formation. Terminal amines from polyamide (PA) are known to react with BIMSM by a nucleophilic substitution reaction to produce BIMSM−PA graft copolymer with a comb-type architecture[28−31] as shown in Figure 1. A non-brominated variety of BIMSM, i.e., only the backbone poly(isobutylene-*co*-*p*-methylstyrene) (IMSM), is apparently incompatible with PA, and no reactions are expected to occur.

Table 1. Material Properties

no.	material	supplier	bromine content (mol %)	M_n	M_w	M_w/M_n	shear rate (s^{-1})
1	IMSM	ExxonMobil	0	226K	530K	2.3	16
2	BIMSM	ExxonMobil	0.75	184K	450K	2.4	16
3	PA 6/6,6	Ube		30K	36K	1.2	89

Only a handful of studies can be found in the literature for the BIMSM/PA system. Yu et al.[31] studied impact properties and found BIMSM very effective in toughing polyamide. Kuwamoto[32] studied the rheology and morphology qualitatively by SEM in noncompatibilized (IMSM/PA), compatibilized (BIMSM/PA), and compatibilized−dynamically vulcanized (BIMSM/PA plus curative) blends. He found the copolymer very effective at reducing the particle size and increasing the interfacial bonding. He also noted composite droplets of PA matrix in elastomer domains. Some other studies[33−35] have examined the addition of nanoclays to BIMSM with PA and other elastomers.

The blends of IMSM/PA and BIMSM/PA offer a nonreactive and reactive reference, respectively, to study the effect of a comb-type graft copolymer on the phase morphology development, interfacial tension, and emulsification of such systems. The detailed study of these phenomena is the principal objective of this paper.

Experimental Procedures

Materials. In this study, IMSM and BIMSM elastomers from ExxonMobil Chemical and a random copolymer of PA 6 (≈85 wt %) and PA 6,6 (≈15 wt %) from Ube Chemical are used. Their molecular weights, molecular weight distributions, composition, along with other material-specific characteristics, and shear rate are summarized in Table 1. Since each polymer material follows different, linear torque vs rotation speed characteristics in an internal mixer, it is more accurate to report the value of the shear rate under actual melt blending conditions individually for each material instead of averaging it for the whole blend. The shear rate values under actual melt blending conditions were estimated by the procedure outlined by Bousmina et al.[36]

Rheological Characterization. The rheological characterization was carried out using a Bohlin constant stress rheometer (CSM) in the dynamic mode. The experiments were performed in a parallel plate geometry of 25 mm diameter and under a nitrogen atmosphere.

Melt Blending. PA, dried overnight, was first dry blended with Irganox 1098, Tinuvin, and CuI stabilizers. The mixture was melt

Table 2. Blend Properties Determined at Constant Shear Rate and Stress[a]

		PA matrix		elastomer matrix	
no.	blend	p^b	Ψ^c	p^b	Ψ^c
1	IMSM/PA	0.5 (0.1)	1.2 (8.3)	1.0 (1.0)	0.4 (0.4)
2	BIMSM/PA	0.4 (0.03)	0.2 (1.7)	1.4 (1.5)	2.9 (2.0)

[a] Values outside parentheses are at constant shear rate and in parentheses are at constant shear stress of the matrix. [b] p = viscosity ratio based on complex viscosity. [c] Ψ = elasticity ratio based on calculated first normal stress difference. The first normal stress difference is estimated using Laun's equation.[37]

mixed in a Brabender internal mixer equipped with 30 cm^3 half-size mixing chamber at 205 °C and 100 rpm and under a nitrogen blanket. The elastomer was fed to the mixing chamber only once the PA was molten. In the emulsification study, IMSM and BIMSM were fed directly into the mixing chamber upon melting of the PA phase. The miscibility of IMSM and BIMSM was confirmed by energy dispersive analysis of X-rays (EDAX) on melt-blended IMSM/BIMSM of different compositions. Morphology analysis indicated no evidence of any phase separation between these elastomers. The mixing was continued, thereafter, for 12 min in the case of blending with IMSM and for the emulsification study and for 3 min in the case of the BIMSM only. In the latter case, it was found that the reaction fixes the morphology very rapidly. After mixing, the melt was quenched quickly in liquid nitrogen to freeze the morphology. The types of blends prepared, as well as their rheological property ratios determined at constant shear rate and stress of the matrix, are reported in Table 2.

Scanning Electron Microscopy (SEM). Samples were cryogenically microtomed using a glass knife to create a plane face. The instrument used was a Leica-Jung RM 2165 equipped with a Leica LN 21 type cryochamber. The elastomer phase was extracted by hexane at room temperature from the microtomed samples in order to improve contrast. However, since very small phases remain unextractable, the use of the SEM was limited to characterizing only the large (>1 μm) domains, i.e., volume-average diameter. The number-average diameter was obtained by atomic force microscopy (AFM).

After drying, the samples were coated with a gold−palladium alloy, and electron micrographs were taken using a Jeol JSM 840 scanning electron microscope operated at a voltage of 15 kV.

Atomic Force Microscopy (AFM). Microtomed specimens were analyzed by tapping mode AFM. Because of the strong modulus contrast between elastomer and PA, tapping phase AFM is an excellent tool in evaluating the morphologies of elastomer/PA blends. The AFM used is equipped with a scanning probe microscope Dimension 3100 with a Nanoscope IIIa or Nanoscope IVa controller from Veeco Instruments. Silicon tips, model RTESP from Veeco and model NCR from Nanoworld, with spring constants of 20−80 N/m and a resonant frequency of approximately 250−350 kHz were used. The tip was oscillated at approximately 98% of the resonant frequency. Topological, phase, and amplitude pictures were taken at 40−70% of the free oscillation amplitude.

Image Analysis. The micrographs obtained were analyzed using a semiautomatic method of image analysis consisting of Adobe Photoshop and Image Processing Tool Kit (IPTK) plug-in available from Reindeer Graphics. On average, at least 500 diameters were measured per blend sample. The number-average diameter (d_n) and volume-average diameter (d_v) were calculated on the basis of these measurements. Since the microtoming plane might not cut the particles at their equator and to correct for polydispersity of the specimens, Saltikov corrections[38] were applied to these measurement. An excellent correlation is obtained between the values determined using this technique and our in-house semiautomatic method of image analysis, consisting of a digitizing table and SigmaScan Pro software, described elsewhere.[39]

Breaking-Thread Technique. The breaking-thread technique was used to measure the interfacial tension (σ) of the blends as well as the effect of interfacial reactive grafting on the interfacial tension. In these experiments, a PA thread (typically 10−40 μm in diameter) was drawn from the mixture of melt-blended PA and was sandwiched between the two films of the elastomer (typically 500 μm thick). The thread was annealed before and after sandwiching in a vacuum oven at 80 °C in order to relieve any residual stresses. In order to study the effect of interfacial reactive grafting on interfacial tension, the matrix films were made with different concentrations of preblended IMSM and BIMSM.

The sandwich covered with glass slides was then brought to 215 °C and held at that temperature on a Mettler FP 82 HT hot stage and under a nitrogen atmosphere. The capillary instabilities were observed with a Nikon microscope and were recorded directly on the computer with the help of a digital camera. Later, the amplitude (α) was estimated using a Visilog software, and the amplitude growth rate (q) was determined from the slope of the graph of α/R_0 vs time plot, where R_0 is the initial thread radius.

The zero-shear viscosities, necessary in order to determine the interfacial tension from Tomotika's theory,[40] were obtained by fitting the Carreau−Yasuda model to the complex viscosity data obtained upon rheological characterization of the materials at 215 °C. All these values were applied later in the Tomotika equation[40] to obtain a value of the interfacial tension. Each value of interfacial tension reported is an average of at least five measurements done in this way.

Matrix Dissolution. Matrix dissolution was carried out in order to directly observe the shape of the dispersed phase. The samples of the 5 IMSM/95 PA blend were dissolved in formic acid while the samples of the 95 IMSM/5 PA blend were dissolved in hexane at room temperature. Later, the solution was filtered using a 0.8 μm pore size polycarbonate membrane. Subsequently, the specimens were dried and coated by a gold−palladium alloy, and SEM micrographs were taken.

Estimation of the Extent of Copolymer Formed. As mentioned before, hexane is the selective solvent for the elastomer phase and formic acid is the selective solvent for the PA phase. Since these solvents are available for each blend phase, the amount of copolymer produced is determined by extracting the nonreacted fractions from the blend specimen. In this experiment, small specimens weighing ~0.1 g were cut directly from the blend samples. The specimens rich in PA were placed in formic acid while specimens rich in elastomer were placed in hexane, to dissolve nonreacted homopolymers, for more than 3 days. The samples were shaken during this period. Upon extraction, the solution was filtered using a polycarbonate membrane of 0.8 μm pore size. The samples were dried until constant weight is obtained. In the second phase of extraction, the samples previously placed in formic acid were subjected to a hexane wash and vice versa. The same procedure of drying, weighing, and subjecting to another solvent was repeated. In total, each sample was washed twice with formic acid and twice with hexane. The amount of material collected on a membrane was accurately weighed after each solvent wash. The material dissolved in the hexane wash is considered as nonreacted BIMSM, the material dissolved in formic acid is considered as nonreacted PA, and the unextractable material is considered as the copolymer. Gravimetric analysis of all these different blend fractions facilitates the determination of copolymer composition and even the number of grafts/molecule. On average, three specimens at each blend composition were measured in this way with an error of less than 3%.

Results

Microstructure in IMSM/PA Blends. Figure 2 demonstrates AFM and SEM micrographs obtained after dissolving the IMSM phase with hexane at room temperature at various IMSM/PA blend compositions. Though a good correlation is obtained between AFM micrograph (a) and a SEM micrograph (c) for large micrometer-sized domains, the inability of SEM to detect particles below 600 nm diameter is evident in micrograph (b). The micrographs in Figure 2 demonstrate a very wide particle size distribution, and the presence of both large micrometer-sized domains along with very fine nanometer-scale particles

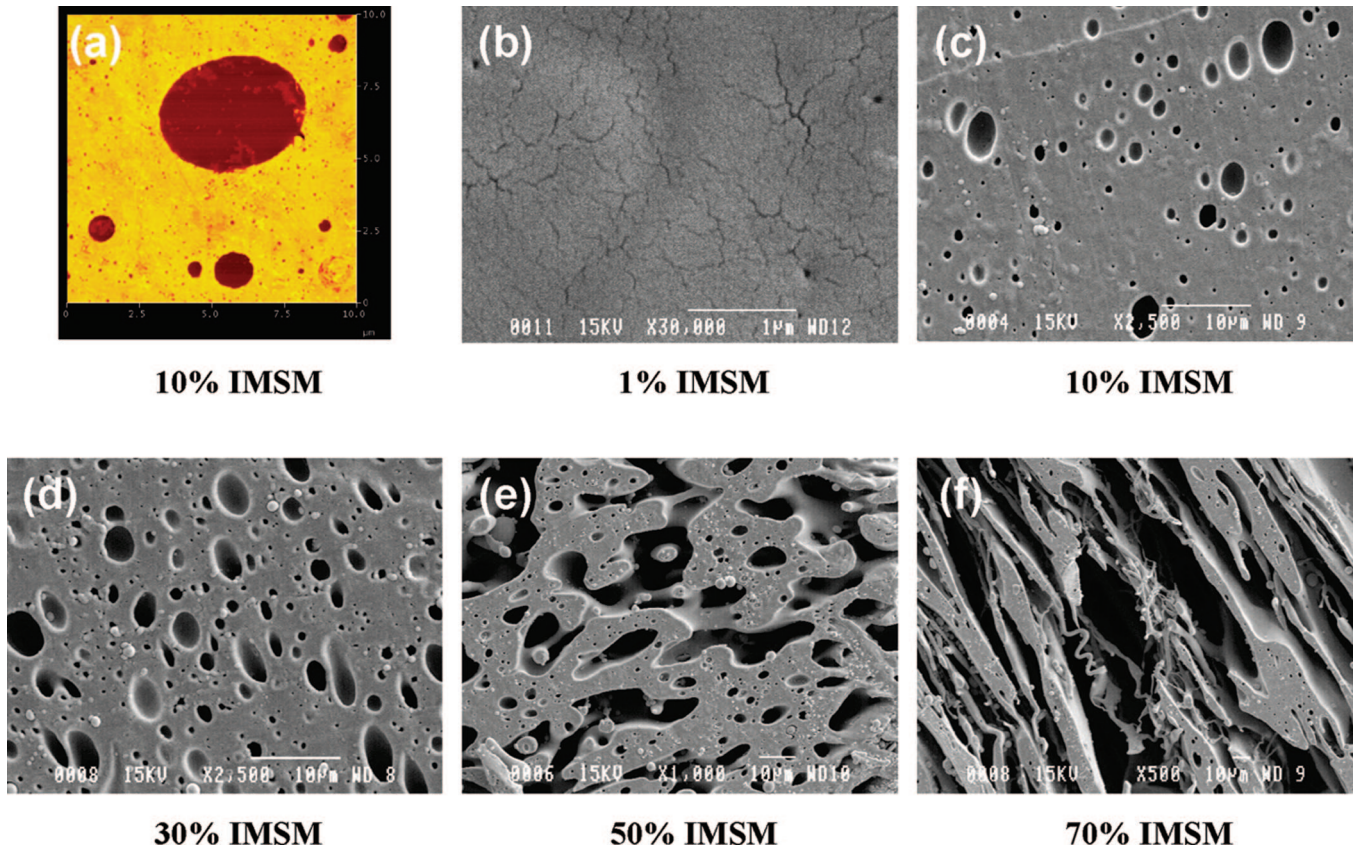

Figure 2. AFM (a) and SEM (b−f) micrographs for the IMSM/PA system. The scale for the AFM micrograph (a) is 10 × 10 μm. White bar is 1 μm for micrograph (b) and 10 μm for micrograph (c−f).

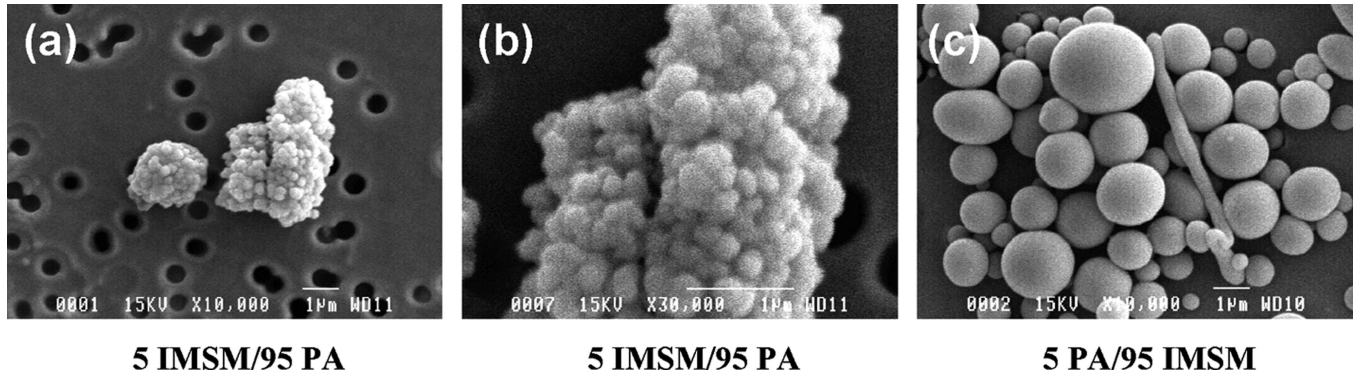

Figure 3. SEM micrographs of the dispersed phase in IMSM/PA blend after matrix dissolution. The white bar indicates 1 μm.

(typically 50−100 nm in diameter) is observed. It is quite unexpected to note these extremely fine, unextractable elastomer domains throughout the entire composition range in such an incompatible system. Wang et al.[30] noted such fine domains of 20−60 nm for pure BIMSM−PS graft copolymer.

Micrograph (e) of Figure 2 at 50% IMSM and micrograph (f) at 70% IMSM demonstrate a cocontinuous morphology and a significant number of elastomer subinclusions in the PA phase is evident. Very few subinclusions of PA were found in the elastomer particles.

SEM micrographs obtained upon matrix dissolution are shown in Figure 3. Such micrographs give important information about the three-dimensional shape of the dispersed microstructures. Micrographs (a) and (b) show an agglomerate of elastomer particles on the membrane surface at different magnifications. Upon removal of the matrix, the elastomer particles tend to agglomerate because of their tackiness as has been observed in other studies.[41,42] Nevertheless, at higher magnification of the elastomer agglomerate, micrograph (b), it can be clearly seen that IMSM exists in the form of spherical particles in the PA matrix. Similarly, spherical PA particles are evident upon dissolution of the elastomer phase in micrograph (c). An occasional occurrence of threads is also evident in the micrograph. Therefore, it can be inferred that the IMSM/PA system demonstrates a low thread frequency ratio[43] at low concentrations of IMSM or PA and that the spherical form for the minor phase dominates over the fiber form during melt mixing. According to the Li et al.[43] nomenclature, these are the typical characteristics of a high interfacial tension (Type II) incompatible system.

Grafting Reaction and Its Effect on Microstructure. Figure 4 shows the torque recorded in the internal mixer for nonreactive IMSM/PA and reactive BIMSM/PA blends at 10% elastomer composition, 100 rpm mixing speed, and at 205 °C mixing temperature. Note that the elastomer is added upon melting of

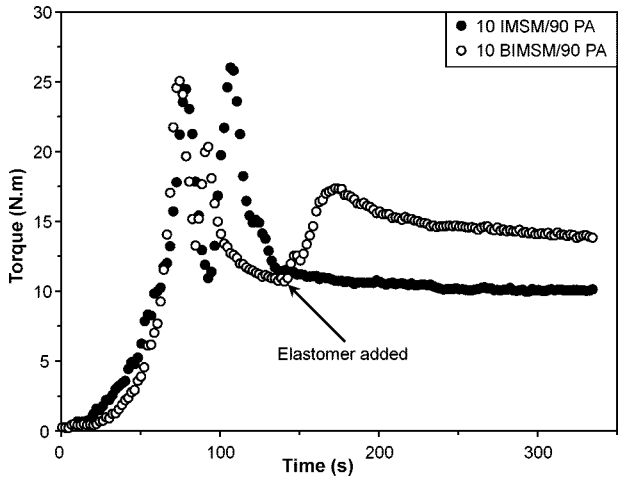

Figure 4. Torque evolution in an internal mixer for IMSM/PA and BIMSM/PA.

PA. Because of the reaction between BIMSM and PA, the torque increases and remains higher than that for the IMSM/PA blend throughout the various blending times. Figure 4 demonstrates that the reaction starts instantaneously and is completed within about a minute. Under optimal reaction conditions and by dissolving the unreacted fractions in selective solvents and weighing the residual material, we estimate that as much as 46 wt % (based on the total weight of the blend) graft copolymer is produced. Overall, in this work we estimate the amount of graft copolymer at each blend composition three times. Additionally, we have also estimated the amount of graft copolymer at each blend composition three times for three different viscosity ratio blends. Similar amounts of graft copolymer are noted, and the error is estimated to be less than 3%. In other work,[44] the formation of a BIMSM−PA graft copolymer was confirmed by FTIR. The spectrum on residual film after PA extraction shows IR peaks associated with both BIMSM and PA and with additional peaks associated with C−N bending and stretching at 800 and 1020 cm^{-1}. Leibler and co-workers[45,46] also reported substantial amounts (35−75 wt %) of graft copolymer formation by increasing the reactivity of the blend components. The yields were measured by size exclusion chromatography (SEC) and selective solvent extraction of ungrafted chains.[45] Yin et al.[47] also reported a similar value of 46 wt % for PS−PMMA graft copolymer.

Figure 5 shows the AFM phase contrast micrographs for reactive BIMSM/PA blends. At low concentrations, extremely fine dispersed domains of BIMSM in a PA matrix are evident in micrograph (a). Particles as small as 40 nm are clearly seen. These morphologies are, arguably, among the finest immiscible phase morphologies reported in the melt-processed polymer blend literature. Moreover, these very fine particles are evident throughout the entire composition range as seen in micrographs (a) to (f). A blown-up version of micrograph (c) in Figure 5 (not shown here) reveals particle−particle interactions but no coalescence to form a single droplet. The graft copolymer at

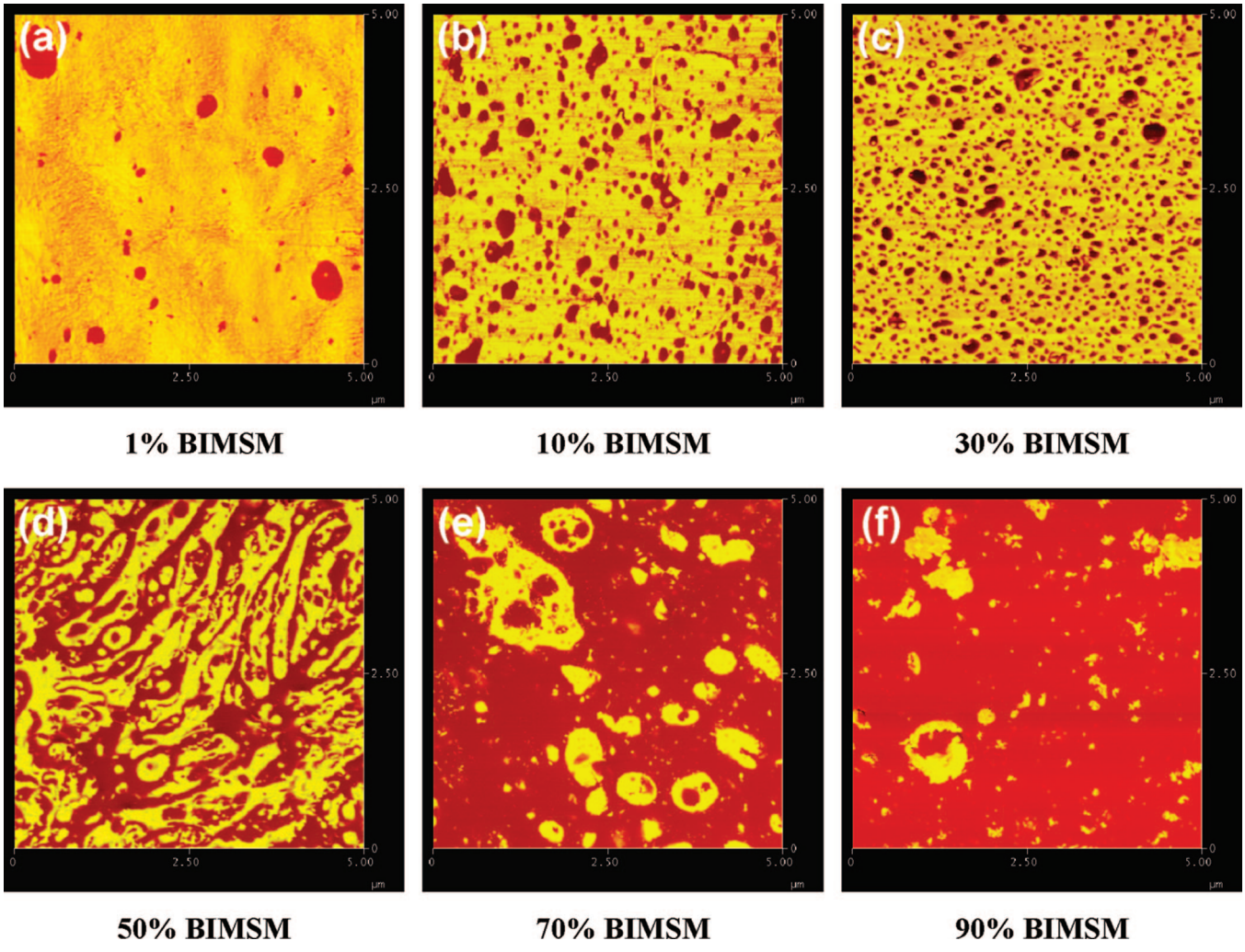

Figure 5. AFM micrographs for the BIMSM/PA system at various concentrations. Scale is 5 × 5 μm for all the micrographs above.

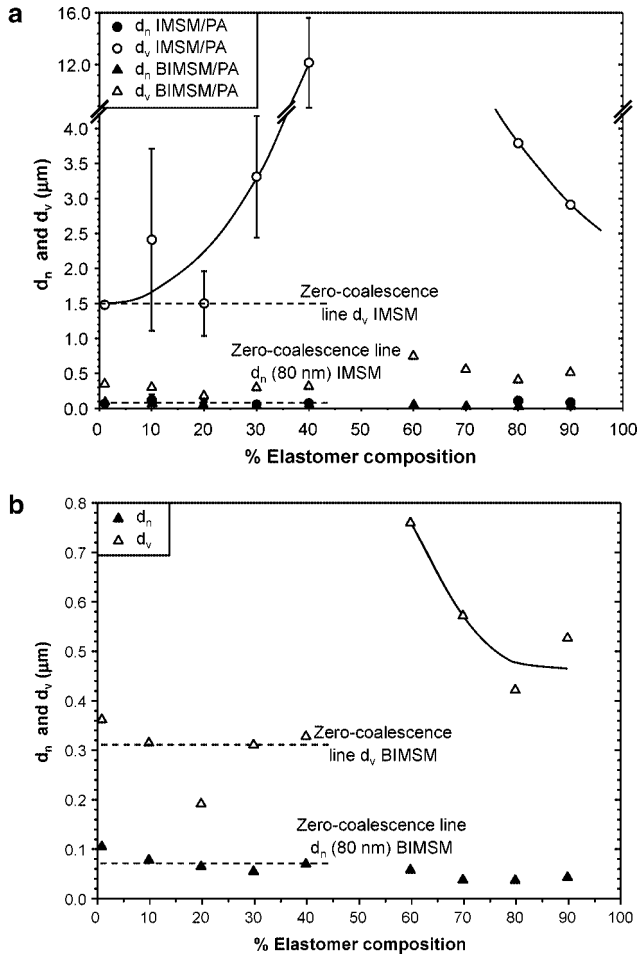

Figure 6. (a) Effect of reactive compatibilization on phase morphology. (b) Particle size/composition diagram for the BIMSM/PA system.

the interface appears very effective in preventing droplet coalescence. This phenomenon will be studied quantitatively in more detail below. With an increase in BIMSM concentration, a cocontinuous morphology is observed, micrograph (d), and significant subinclusions of elastomer in PA, micrographs (d) and (e), are evident. The increase in elastomer concentration results in phase inversion, and dispersed PA particles are evident in micrographs (e) and (f).

Figure 6a demonstrates the results obtained upon phase size analysis of the micrographs in Figures 2 and 5. The number-average diameter (d_n) represents small particles, while the volume-average diameter (d_v) represents larger particles in the blend. Tracking these diameters yield comprehensive information about the blend morphology.

At low concentrations of the dispersed phase, a very wide (15−25-fold) particle size distribution (d_v/d_n) is evident for IMSM/PA blends. This results from the coexistence of extremely fine and very large particles over the entire composition range. Because of coalescence, an increase in d_v is evident for both IMSM and PA phases with an increase in the respective minor phase concentration. The fine particles do not coalesce like the large particles as seen from the zero coalescence lines in the figure.

The effect of reactive compatibilization on the phase morphology of the BIMSM/PA system is plotted in Figure 6a together with the nonreactive IMSM/PA and also separately in Figure 6b. The similarity in the d_n values for both IMSM/PA and BIMSM/PA suggests some low level of reactivity is also present in the IMSM/PA system. At 1% BIMSM, no coalescence is expected, and a corresponding zero coalescence baseline is drawn in the figure. At that low concentration, the diminished phase size for BIMSM/PA as compared to IMSM/PA should be directly related to the drop in interfacial tension,[12] and a 5-fold drop in d_v is evident. The BIMSM/PA blend also shows no change in either d_n or d_v with increasing composition over the entire composition range, a clear indication that the coalescence of droplets is entirely suppressed. The particle size distribution (d_v/d_n) for BIMSM/PA is about three, and that high distribution is maintained right up to the region of dual phase continuity (50% BIMSM). In the literature, the effective interfacial modification of a blend system almost always results in significantly lower particle size distributions between 1 and 1.5. Also, at 40% BIMSM concentration, this reactive compatibilization protocol results in a massive 37-fold drop in volume average diameter particle size as compared to that for IMSM/PA. Even after accounting for highly effective coalescence suppression and interfacial tension reduction,[5,7,8,12−15,48] it is impossible to fully explain this spectacular drop in phase size. A new model explaining the above anomalies along with the detailed discussion of differences from the other studies demonstrating similar results is given later in the Discussion section.

Table 3. Effect of Copolymer Formation on Interfacial Tension by Breaking-Thread Measurements

no.	matrix composition	σ(mN/m)
1	100% IMSM	0.6−3.2
2	98% IMSM/2% BIMSM	1.6−3.6
3	95% IMSM/5% BIMSM	no breakup
4	80% IMSM/20% BIMSM	no breakup

Effect of Copolymer on Interfacial Tension. The value of interfacial tension (σ) obtained between IMSM and PA by the breaking-thread technique and the effect of graft copolymer concentration on interfacial tension are summarized in Table 3 and Figure 7. The zero shear viscosities were obtained by extrapolation of the viscosity/shear rate data using the Carreau−Yassuda equation (Figure 7a) and as outlined in the Experimental Procedures. Typical sinusoidal distortions were observed (Figure 7b−e). The plot of the distortion amplitude versus time is shown in Figure 7f, and the expected linear behavior is observed. Even under carefully controlled conditions, the value of interfacial tension between IMSM and PA is found to be in between 0.6 and 3.2 mN/m. Over a wide range of studies from this laboratory,[12,15] the typical variation in interfacial tension results from the breaking-thread technique is about 10%. This large variation is a further indication of some low level of reactivity present in the IMSM/PA system.

It is very interesting to note the dramatic effect of interfacial graft copolymer on interfacial tension (see Table 3). A small amount of interfacial graft copolymer, only 5%, reduces the interfacial tension so significantly that no thread breakup is observed. Clearly, the comb-type BIMSM−PA graft copolymer is very effective at reducing the interfacial tension. In some cases, production of copolymer produced at the interface during a breaking-thread experiment could potentially migrate into the dispersed phase or matrix. In the current study, however, if this were occurring, it would indicate that even lower concentrations of copolymer are required to reduce interfacial tension and not greater values.

Emulsification Study. An emulsification study examining the effect of the amount of graft copolymer on particle size was undertaken. The literature has shown that the emulsification curve is an important tool in investigating and understanding the effectiveness of a given copolymer as an emulsifier. In this study, since the copolymer is produced in situ right at the interface, the copolymer concentration is controlled by varying the concentration of the reactive BIMSM elastomer to the

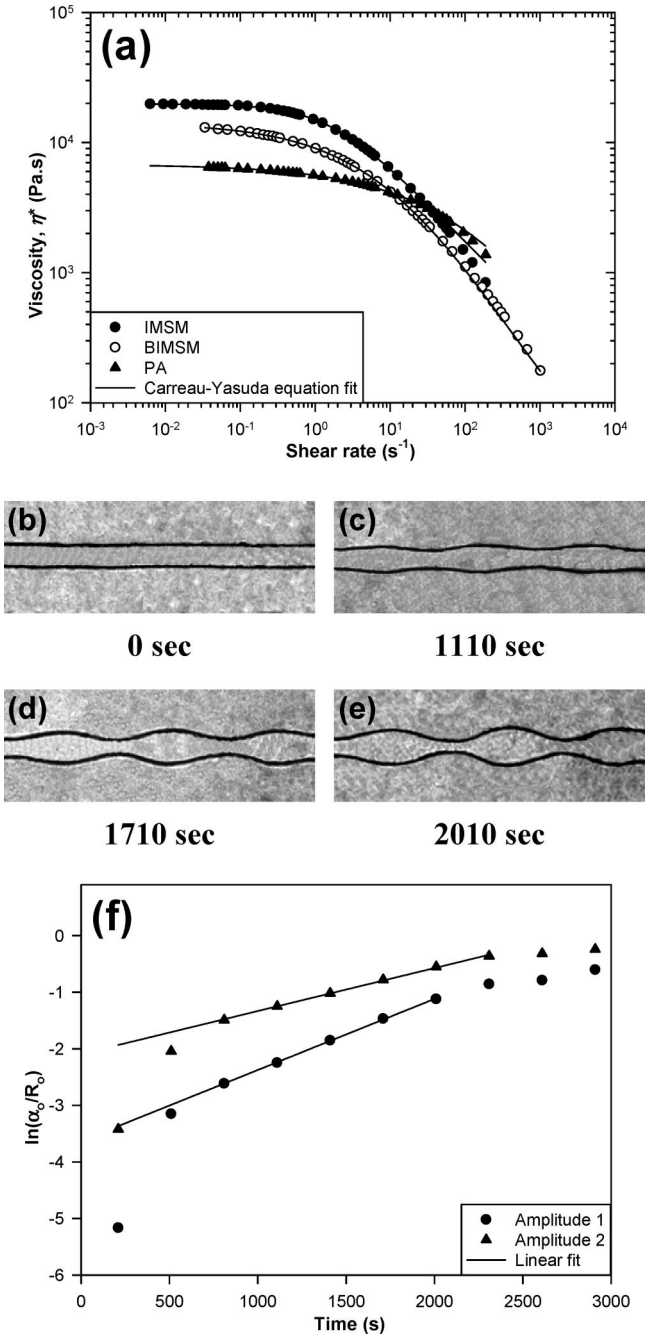

Figure 7. Breaking thread results for interfacial tension measurement at 215 °C. (a) Viscosity curves and zero-shear viscosity estimation. (b−e) Sinusoidal distortions of PA thread. (f) Increase of distortion amplitude with time.

nonreactive IMSM elastomer. A fixed blend composition of 10 parts of elastomer to 90 parts of PA was used.

The AFM phase contrast micrographs at different concentrations of copolymer are shown in Figure 8. The micrographs effectively demonstrate the gradual increase in the number of fine particles and the decrease in particle size of the large particles with increasing amount of copolymer up to 20 IMSM/80 BIMSM (micrograph (e)).

The quantitative image analysis of these micrographs is shown in Figure 9. As observed throughout this article, no change in d_n is evident with the amount of copolymer. However, the volume average diameter, d_v, decreases linearly up to 20 IMSM/80 BIMSM concentration. Normally, copolymer concentrations of 10−20%, based on the dispersed phase, are sufficient to fully saturate an interface in an immiscible binary polymer blend.[7,8,12−14,49] Li et al.[49] reported that 12.5% of copolymer (based on the dispersed phase) was required to saturate 580 nm diameter particles, close to the size scale observed here. However, in this case the lower limiting particle size is only achieved at the 20 IMSM/80 BIMSM concentration. At that concentration the amount of BIMSM based on IMSM is 400%, which clearly places it outside the realm of a simple interfacial saturation argument. This anomalous behavior is even more difficult to explain when one considers that the amount of copolymer necessary to completely inhibit breakup in the static interfacial tension experiment was only 95% IMSM/5% BIMSM.

Discussion

In this paper several important anomalies have been observed for the reactive BIMSM/PA system as compared to other classical interfacially modified systems. These anomalies are as follows: (1) as much as a 37-fold reduction in d_v for the reactive system as compared to the nonreactive one; (2) high d_v/d_n phase size distributions at all blend compositions and at all copolymer concentrations with the fine droplets being in the 50−80 nm range scale; (3) extensive droplet in droplet formation for BIMSM in PA in a BIMSM matrix; (4) very high extents of reaction, 46% of the total blend material reacts over a short time of mixing; (5) a continuous linear drop in elastomer phase size with increase in copolymer concentration to produce fine nanoscale droplets as a function of IMSM/BIMSM content. This is well beyond the amount of copolymer needed to saturate the interface even though static interfacial tension studies show that only 5% BIMSM in IMSM completely suppresses capillary breakup.

On the basis of the chemical composition and average molecular weight as reported in Table 1, it is estimated that, on average, there are 38 potential bromine sites available for reactive grafting with PA per BIMSM molecule. When the BIMSM backbone reacts with PA, it clearly has the potential for reaction at multiple sites and under those conditions would form a comb-type copolymer (BIMSM backbone with multiple PA teeth). If we consider the monomer length (l) of isobutylene (the backbone for BIMSM) as 0.252 nm and that for PA as 0.882 nm and degrees of polymerization (n) of 5050 and 292, respectively, one can estimate a minimum radius of gyration (R_g) for BIMSM of about 7 nm for BIMSM and 6 nm for the PA chain using the following equation:

$$R_g = \left(\frac{nl^2}{6}\right)^{1/2}$$

On the basis of those dimensions, a BIMSM backbone with multiple PA teeth would clearly fall into the same order of magnitude of dimensions of the finest particles in the system (about 50 nm) and would support an explanation that the fine particles (d_n) are actually micelles of the reacted graft copolymer. Moreover, as mentioned previously, Wang et al.[30] observed fine domains of 20−60 nm for pure BIMSM−PS graft copolymer and noted that the fine particles (below 600 nm) are unextractable in hexane, a solvent for BIMSM. This further supports the above conclusion.

The self-assembly of copolymers into a variety of well-organized nanoscale micelle structures, e.g. spheres, cylinders, vesicles, etc., and their use in nanodevices is well-known in the literature.[50−52] The final structure of the assembly mainly depends on the chemical composition, functionality, and the architecture of the copolymer. In the case of a linear comb architecture copolymer the simplest form is a spherical core−shell micelle, consisting of a core of backbone molecules and a shell of the various teeth grafted onto a backbone. In the case of the present system, this translates to a BIMSM elastomer core and a PA shell. Indeed,

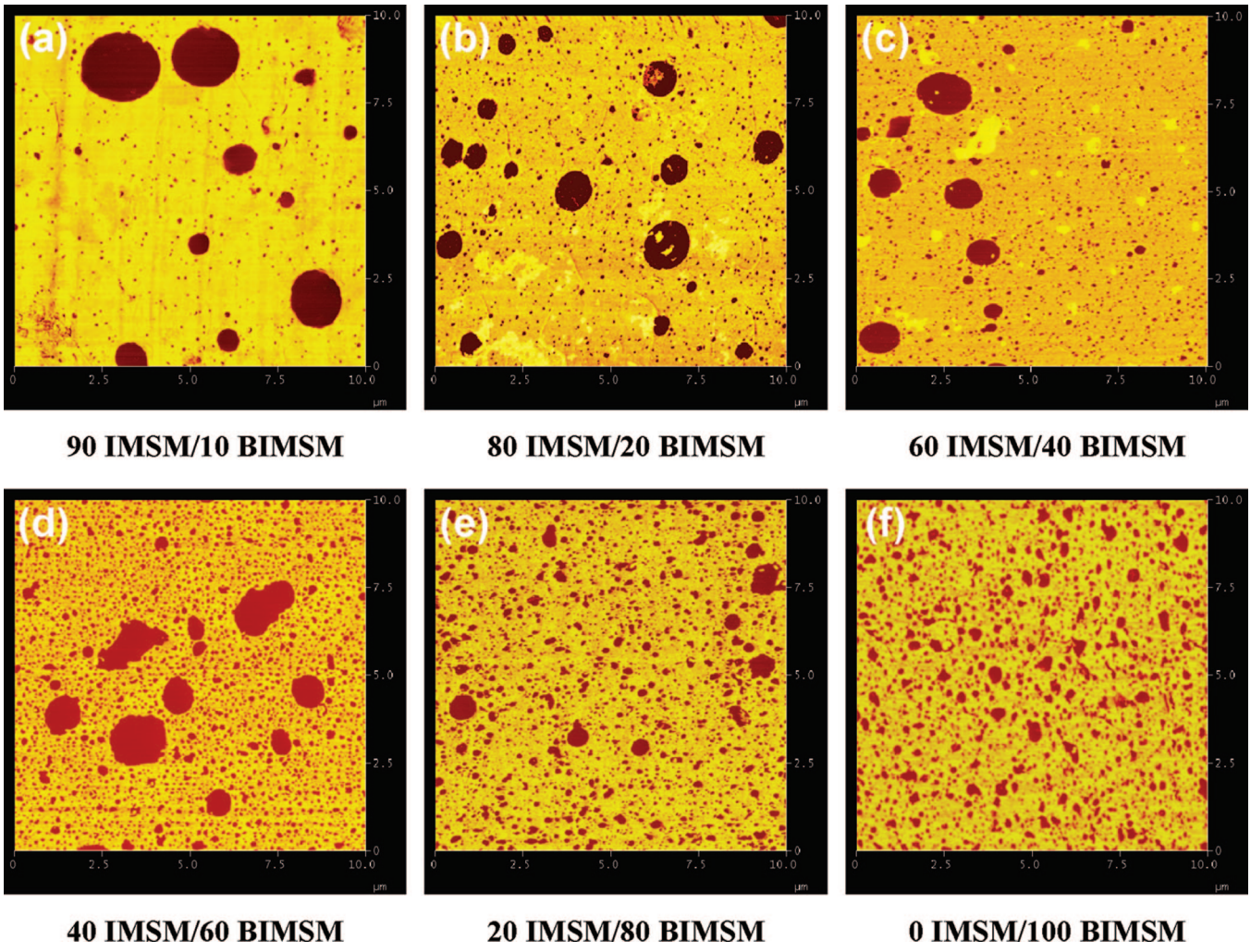

Figure 8. Emulsification study of 10 (IMSM/BIMSM)/90 PA blends. Scale is 10 × 10 μm for all the micrographs above.

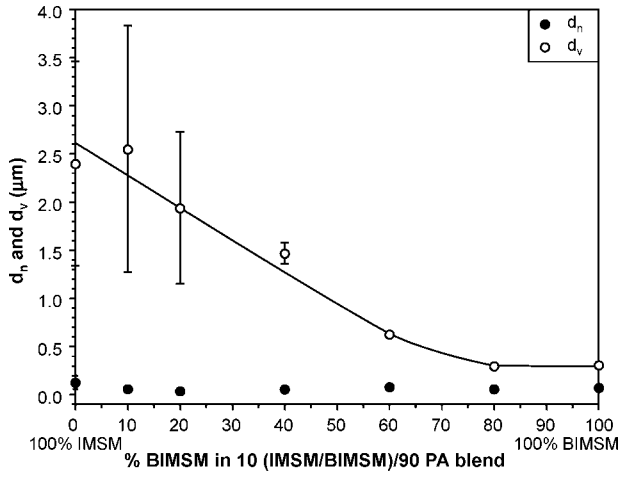

Figure 9. Emulsification curve for 10 (IMSM/BIMSM)/90 PA blends.

such a structure would explain the presence of nanoscale micelles at lower BIMSM concentrations and subinclusions of elastomer in PA at mid and higher BIMSM concentrations.

Interfacial Erosion Mechanism of Morphology Development. In order to explain how the micelles of graft copolymer form in the first place, we describe here a novel mechanism termed "interfacial erosion". The mechanism considers the formation of a graft copolymer right at the interface during dynamic mixing, resulting from the mutual contact of the BIMSM and PA molecules, and its subsequent departure from the interfacial region to form fine, nanometer-sized micelles in the bulk. The removal of the copolymer from the interface exposes nonreacted material and primes the interfacial region for further copolymer formation. In this fashion, most of the BIMSM can be made to react, and the resulting blend is a nanoscale dispersion with a size scale (d_n) in the order of 50−80 nm.

Figure 10 shows high-magnification micrographs of BIMSM/PA blends. The circles points to areas where there is a clear tendency of the extreme outer shell of the BIMSM to break away from the main dispersed phase. The portions breaking away are typically in the "less than 100 nm" scale range. The mechanism is conceptually described in more detail below.

The mutual contact between the pendent bromine of the BIMSM and the amine end group of the polyamide results in the almost instantaneous formation of graft copolymer according to Figure 11a. Since each BIMSM molecule carries 38 potential sites for grafting, multiple grafting at the interface results in a comblike graft copolymer architecture as shown in the schematic in Figure 11b. Upon exceeding a critical number of PA grafts, the BIMSM−PA copolymer leaves the interface to migrate into the PA bulk phase as shown in Figure 11c. The removal of the copolymer from the interface exposes nonreacted material and primes the interfacial region for further copolymer formation.

Theoretically, Balazs and co-workers[20−24] have shown that higher molecular weight comb copolymers and a number of teeth corresponding to a symmetric comb composition are the

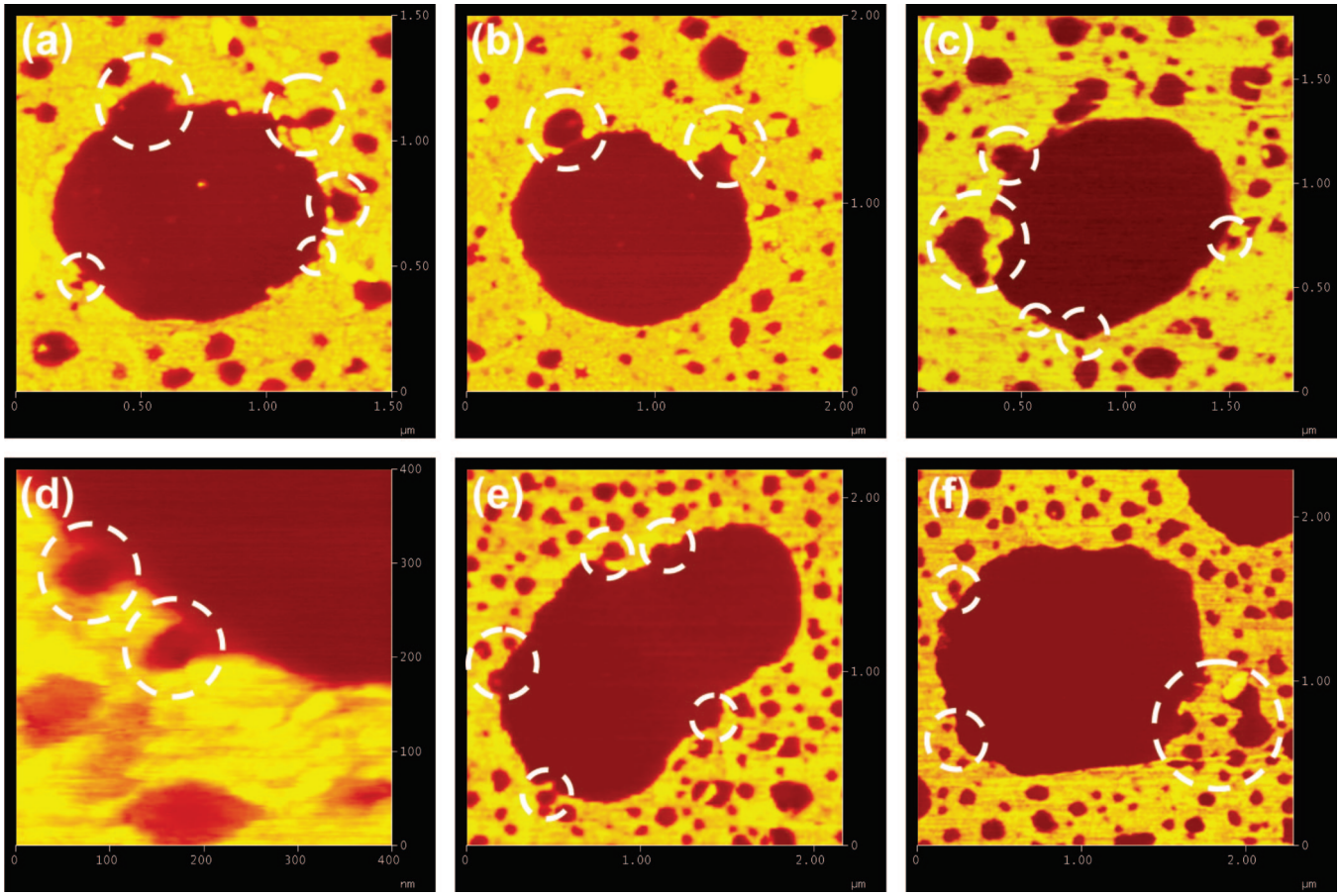

Figure 10. Micrographs depicting interfacial erosion in the BIMSM/PA system. Scale is: (a) 1.5 × 1.5 μm; (b) 2.0 × 2.0 μm; (c) 1.8 × 1.8 μm; (d) 400 × 400 nm; (e) 2.1 × 2.1 μm; (f) 2.3 × 2.3 μm.

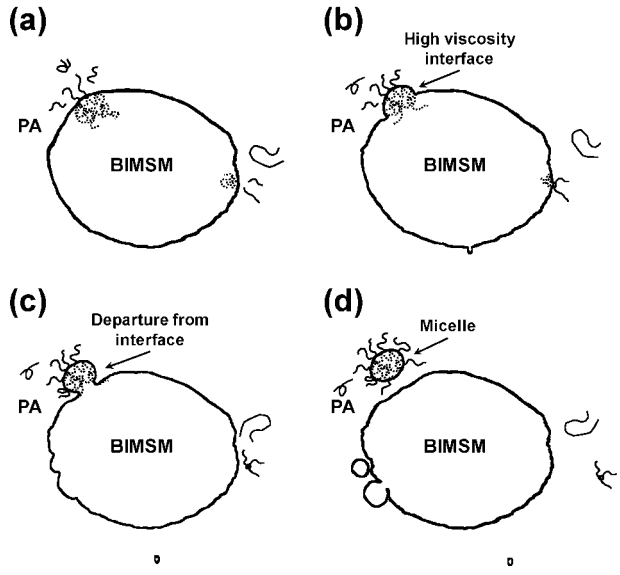

Figure 11. Schematic of interfacial erosion mechanism of morphology development.

most effective at reducing interfacial tension. Considering the molecular weights of the components in the present study (see Table 1), a symmetric composition will be achieved at nine PA grafts. Further grafting above this level will lead to a copolymer rich in PA and from a thermodynamic point of view would justify its departure away from the interface to the bulk PA phase. The quantity of copolymer produced during the reactive protocol used in this work was determined using selective solvents for both BIMSM and PA, as explained in the Experimental Procedures. At optimal reaction conditions, the results show that more than 46 wt % of the blend material (30 wt % BIMSM and 16 wt % PA) participates in the reaction. This can be interpreted to result in seven (based on M_w) to at least three to four (based on M_n) PA grafts per BIMSM molecule. These results point to a comb copolymer formation in the present work that would always be rich in BIMSM. Therefore, the copolymer departure from the interface does not appear to be thermodynamically driven.

A number of studies in the literature have reported on the presence of nanoscale morphologies in reactive polymer blending. Majumdar et al.[53] and Dedecker et al.[54] observed the formation of nanoscale micelles resulting from the phase separation of in situ formed graft copolymer resulting from the reaction of imidized acrylic polymers and styrene−maleic anhydride, respectively, with PA. They showed that their reactive compatibilizing agent demonstrates a miscibility window according to the concentration of functional groups. Within the miscibility limits, the compatibilizing agent was successful in emulsifying the blend system and demonstrated typical morphologies. Near or outside the limits of miscibility, however, the compatibilizing agent failed to compatibilize the system and phase separated to form nanoscale micelles in the matrix. In that study, however, there is no interfacial erosion, as in the present work, and the micelles clearly result from miscibility issues.

In a pioneering study, Leibler and co-workers[46] demonstrated that through a meticulous control of molecular weight, polydispersity, random graft attachment, and distance between grafts, maleic anhydride grafted polyethylene and PA blends could result in thermodynamically stable, nanoscale sized cocontinuous morphologies by reactive blending. This control generated

symmetric copolymer molecules which dissolve low molecular weight unreacted chains and self-assemble to form interfaces with large radii of curvature. The asymmetric copolymers obtained by reducing the number of reactive sites on the backbone failed to dissolve unreacted chains driving the system to phase separate into nanoscale micelles and macrophases.

Kim et al.[55,56] studied the temporal change of the complex viscosity of two layered reactive polymers in a parallel plate rheometer at extremely low shear rates. They found three distinct stages in the viscosity behavior with time. Initially (stage I) the viscosity increased rapidly with time and attained a plateau value (stage II). Later (stage III) the viscosity increased again and reached a final value. In the later stages they observed an increase in the interface roughness with reaction and spontaneous pinching to form nanoscale micelles at very long times (4−17 h). This work is interesting since it supports the notion of nanoscale micelles forming from high viscosity interfaces; there are, however, major differences between that work and the present study. In the current work, interfacial erosion is observed as occurring from a discrete dispersed phase in a reactive blend system prepared in an internal mixer after 3−12 min of mixing.

Inoue and co-workers[57−59] observed a chain pull-out of in situ formed copolymer under the dynamics of melt processing. The molecular weights of the copolymers they studied were in the range of 5K to at most 70K. They found that the aggressive hydrodynamic conditions generated by melt processing play a more important role in the chain pull-out process over thermodynamics. Present theories on polymer interfaces based on thermodynamics deal with chain statistics in the quiescent state and do not consider the disruptive extreme conditions of melt processing. They observed that the block copolymers with linear chain architecture and graft copolymers having trunk chains located in the matrix are easily pulled out to form micelles in the matrix. The rapid reaction kinetics leading to an excess accumulation of the copolymer at the interface also played a crucial role in the process. The graft copolymers having trunk chains located in the dispersed phase were more difficult to remove; however, strong shear fields successfully pulled them out from the interface. An asymmetric comb architecture generated by grafting multiple teeth, each of which had a molecular weight comparable to the backbone, was successfully pulled out into the phase representing the dominant composition in the copolymer. Compared to the above study, the molecular weights in the present work are several times higher, especially that of the backbone BIMSM. Molecular entanglement effects would thus be expected to be much more important in our system. Furthermore, in the current study, the interfacial erosion of dispersed BIMSM and the subsequent micelle formation of reacted copolymer occur in the PA matrix, which is the by far the least dominant composition in the copolymer. This suggests that a different physical phenomenon must be dominating the morphology development in the present system.

The mechanism operating in the current work will now be considered in more detail. The increase in molecular weight and chain branching is known in the literature to significantly increase the viscosity of the polymer.[2,60−62] In the case of a comb copolymer grafting reaction, the subsequent chain branching would be expected to increase the viscosity even more than the sum of the viscosities of the two reacting polymers. Therefore, in this case, seven branches of PA on a single BIMSM molecule would be expected, at a minimum, to increase the viscosity of the copolymer by 8-fold. The in situ graft reaction, therefore, results in the formation of a very high viscosity interfacial region. This viscosity mismatch between the copolymer at the interface and the base components of the blend, during melt mixing, would tend to pull the copolymer away from the interface along with entangled molecules. Our previous work on the dynamic vulcanization[63] and high viscosity ratio blends of low interfacial tension[42] demonstrated a similar erosion and smearing process of the interfacial region.

The removal of the copolymer to form micelles in the bulk exposes a fresh interface for further reaction, as shown in the schematic in Figure 11d. In this fashion, the BIMSM and the PA continue to react until most of the BIMSM is consumed. Unreacted entangled material departing with graft copolymer from the interface could also further react and erode into fine micelles. Also, since the grafting reaction kinetics between BIMSM and PA are very rapid,[44,64] the excess accumulation of copolymer at the interface might also accelerate the interfacial erosion process in the case of high BIMSM/low IMSM concentration blends with PA.

Undoubtedly, in parallel to this interfacial erosion, the usual droplet breakup mechanisms will also proceed. Nevertheless, the interfacial erosion clearly determines the final morphology. This is due to the continuous production of fresh interface which never allows for the formation of a stable interfacial layer surrounding unreacted material as is typically observed in compatibilized polymer blend systems.

The above mechanism effectively explains all the anomalous experimental features observed in this study including the following: the massive 37-fold drop in phase size observed in the 40 BIMSM/60 PA blend; the high particle size distribution; the extensive droplet in droplet formation for BIMSM in PA in a BIMSM matrix; the very high extent of reaction over a short time of mixing; and the continuous linear drop in elastomer phase size with IMSM/BIMSM content during mixing up to 20 IMSM/80 BIMSM, well beyond the amount of copolymer needed to saturate the interface even though static interfacial tension studies show that only 5% BIMSM in IMSM completely suppresses capillary breakup.

This work, therefore, emphasizes the importance of taking into consideration the aggressive hydrodynamic effects related to melt mixing. It also raises important considerations concerning the use of graft copolymers, in general, in polymer blend systems. Clearly, graft copolymer strategies, which are a central theme in industrial reactive processing protocols, will need to take into account the possibility of phase morphology generation via interfacial erosion.

Conclusions

In this work, the morphology development and the effects of reactive compatibilization on the blend morphology of IMSM and BIMSM elastomer with PA are investigated. The nonreactive IMSM/PA blends demonstrate several typical characteristics of a high interfacial tension system including micrometer-sized, large spherical particles, and significant particle−particle coalescence with increase in concentration. However, the blends also demonstrate the presence of a small quantity of extremely fine, micelle sized (50−80 nm) particles, which suggest some low-level reactivity between IMSM and PA.

The reaction between pendent benzylic bromine in BIMSM and the terminal amine in PA results in a BIMSM−PA graft copolymer with a linear comb-type architecture. The protocol produces as much as 46 wt % graft copolymer, based on the total weight of the blend, with as many as seven PA grafts per BIMSM molecule. The reactive compatibilization effectively suppresses the particle−particle coalescence in the system and, depending upon the concentration, reduces the particle size anywhere from 5- to 37-fold. The particle size distribution (d_v/d_n) of the reactive system is high at about three.

An emulsification study at 10 elastomer/90 PA composition demonstrates a linear drop in particle size and requires a very high concentration of copolymer (20 IMSM/80 BIMSM) to

reach a plateau value. This is well beyond the amount of copolymer needed to saturate the interface since the static interfacial tension studies show that only 5% BIMSM in an IMSM matrix completely suppresses capillary breakup. The above anomalies are explained by a novel mechanism of morphology development during dynamic melt mixing termed "interfacial erosion".

The mechanism considers the formation of a very high viscosity comb-type graft copolymer right at the interface resulting from the mutual contact of the BIMSM and PA molecules. However, the viscosity mismatch between the graft copolymer and the base components of the blend leads to the erosion of the interface region, during dynamic melt mixing, to form fine, nanometer-sized micelles in the bulk. The removal of the copolymer from the interface exposes nonreacted material and primes the interfacial region for further copolymer formation. In this fashion, most of the BIMSM can be made to react, and the resulting blend transits to a nanoscale dispersion.

References and Notes

(1) Utracki, L. A. *Polymer Blends Handbook*, 1st ed.; Kluwer Academic Publishers: Dordrecht, 2002.
(2) Hadjichristidis, N.; Pispas, S.; Pitsikalis, M.; Iatrou, H.; Lohse, D. J. In *Encyclopedia of Polymer Science and Technology*, 3rd ed.; Mark H. F., Ed.; John Wiley & Sons: New York, 2002; Vol. *6*, pp 349−385.
(3) Creton, C.; Kramer, E. J.; Hadziioannou, G. *Macromolecules* **1991**, *24*, 1846–1853.
(4) Peiffer, D. G.; Rabeony, M. *J. Appl. Polym. Sci.* **1994**, *51*, 1283–1289.
(5) Polizu, S.; Favis, B. D.; Vu-Khanh, T. *Macromolecules* **1999**, *32*, 3448–3456.
(6) Noolandi, J.; Hong, K. M. *Macromolecules* **1982**, *15*, 482–492.
(7) Matos, M.; Favis, B. D.; Lomellini, P. *Polymer* **1995**, *36*, 3899–3907.
(8) Cigana, P.; Favis, B. D.; Jerome, R. *J. Polym. Sci., Polym. Phys.* **1996**, *34*, 1691–1700.
(9) Lyu, S.; Jones, T. D.; Bates, F. S.; Macosko, C. W. *Macromolecules* **2002**, *35*, 7845–7855.
(10) Tan, N. C.; Tai, S. K.; Briber, R. M. *Polymer* **1996**, *37*, 3509–3519.
(11) Milner, S. T.; Xi, H. *J. Rheol.* **1996**, *40*, 663–687.
(12) Lepers, J. C.; Favis, B. D. *AIChE J.* **1999**, *45*, 887–895.
(13) Elemans, P. H. M.; Janssen, J. M. H.; Meijer, H. E. H. *J. Rheol.* **1990**, *34*, 1311–1325.
(14) Chen, C. C.; White, J. L. *Polym. Eng. Sci.* **1993**, *33*, 923–930.
(15) Chapleau, N.; Favis, B. D.; Carreau, P. J. *J. Polym. Sci., Polym. Phys.* **1998**, *36*, 1947–1958.
(16) Leibler, L. *Makromol. Chem., Macromol. Symp.* **1988**, *16*, 1–17.
(17) Shull, K. R.; Kramer, E. J.; Hadziioannou, G.; Tang, W. *Macromolecules* **1990**, *23*, 4780–4787.
(18) Brown, H. R.; Char, K.; Deline, V. R.; Green, P. F. *Macromolecules* **1993**, *26*, 4155–4163.
(19) Arlen, M. J.; Dadmun, M. D. *Polymer* **2003**, *44*, 6883–6889.
(20) Lyatskaya, Y.; Gersappe, D.; Balazs, A. C. *Macromolecules* **1995**, *28*, 6278–6283.
(21) Lyatskaya, Y.; Jacobson, S. H.; Balazs, A. C. *Macromolecules* **1996**, *29*, 1059–1061.
(22) Gersappe, D.; Harm, P. K.; Irvine, D.; Balazs, A. C. *Macromolecules* **1994**, *27*, 720–724.
(23) Israels, R.; Foster, D. P.; Balazs, A. C. *Macromolecules* **1995**, *28*, 218–224.
(24) Yilgor, I.; Yilgor, E.; Venzmer, J.; Spiegler, R. *Interfacial Aspects Multicompon. Polym. Mater.* **1977**, 195–209.
(25) Majumdar, B.; Paul, D. R. In *Polymer Blends: Formulations*; Paul, D. R., Bucknall, C. B., Eds.; John Wiley & Sons: New York, 2000; Vol. *1*, Chapter 17, pp 539−579.
(26) Macosko, C. W. *Macromol. Symp.* **2000**, *149*, 171–184.
(27) Macosko, C. W.; Jeon, H. K.; Hoye, T. R. *Prog. Polym. Sci.* **2005**, *30*, 939–947.
(28) Powers, K. W.; Wang, H. C.; Chung, T. C.; Dias, A. J.; Olkusz, J. A. US Patent 5,162,445, **1992**.
(29) Wang, H. C.; Powers, K. W. *Elastomerics* **1992**, *124*, 14–19.
(30) Wang, H. C.; Powers, K. W. *Elastomerics* **1992**, *124*, 22–24.
(31) Yu, T. C.; Wang, H. C.; Powers, K. W.; Yee, A. F.; Li, D. *Polym. Prepr.* **1992**, *33*, 622–623.
(32) Kuwamoto, K. *Int. Polym. Process.* **1994**, *9*, 319–325.
(33) Maiti, M.; Sadhu, S.; Bhowmick, A. K. *J. Polym. Sci., Polym. Phys.* **2004**, *42*, 4489–4502.
(34) Maiti, M.; Bandyopadhyay, A.; Bhowmick, A. K. *J. Appl. Polym. Sci.* **2006**, *99*, 1645–1656.
(35) Tsou, A. H.; Measmer, M. B. *Rubber Chem. Technol.* **2006**, *79*, 281–306.
(36) Bousmina, M.; Ait-Kadi, A.; Faisant, J. B. *J. Rheol.* **1999**, *43*, 415–433.
(37) Laun, H. M. *J. Rheol.* **1986**, *30*, 459–501.
(38) Saltikov, S. A. In *Proceedings of the Second International Congress for Stereology*; Elias, H., Ed.; Springer-Verlag: Berlin, 1967; pp 163−173.
(39) Favis, B. D.; Chalifoux, J. P. *Polym. Eng. Sci.* **1987**, *27*, 1591–1600.
(40) Tomotika, S. *Proc. R. Soc. London* **1935**, *A150*, 322–337.
(41) Bhadane, P. A.; Champagne, M. F.; Huneault, M. A.; Tofan, F.; Favis, B. D. *Polymer* **2006**, *47*, 2760–2771.
(42) Bhadane, P. A.; Champagne, M. F.; Huneault, M. A.; Tofan, F.; Favis, B. D. *J. Polym. Sci., Polym. Phys.* **2006**, *44*, 1919–1929.
(43) Li, J.; Ma, P. L.; Favis, B. D. *Macromolecules* **2002**, *35*, 2005–2016.
(44) Tsou, A. H.; Favis, B. D.; Hara, Y.; Bhadane, P. A.; Kirino, T. Manuscript in preparation.
(45) Freluche, M.; Iliopoulos, I.; Milléquant, M.; Flat, J.; Leibler, L. *Macromolecules* **2006**, *39*, 6905–6912.
(46) Pernot, H.; Baumert, M.; Court, F.; Leibler, L. *Nat. Mater.* **2002**, *1*, 54–58.
(47) Yin, Z.; Koulic, C.; Pagnoulle, C.; Jérome, R. *Macromolecules* **2001**, *34*, 5132–5139.
(48) Anastasiadis, S. H.; Gancarz, I.; Koberstein, J. T. *Macromolecules* **1989**, *22*, 1449–1453.
(49) Li, J.; Favis, B. D. *Polymer* **2002**, *43*, 4935–4945.
(50) Abetz, V. In *Encyclopedia of Polymer Science and Technology*, 3rd ed.; Mark, H. F., Ed.; John Wiley & Sons: New York, 2002; Vol. *1*, pp 482−523.
(51) Riess, G. *Prog. Polym. Sci.* **2003**, *28*, 1107–1170.
(52) Ikkala, O.; ten Brinke, G. *Chem. Commun.* **2004**, 2131–2137.
(53) Majumdar, B.; Keskkula, H.; Paul, D. R.; Harvey, N. G. *Polymer* **1994**, *35*, 4263–4279.
(54) Dedecker, K.; Groeninckx, G. *Polymer* **1998**, *39*, 4985–4992.
(55) Kim, H. Y.; Jeong, U.; Kim, J. K. *Macromolecules* **2003**, *36*, 1594–1602.
(56) Kim, H. Y.; Ryu, D. Y.; Jeong, U.; Kho, D. H.; Kim, J. K. *Macromol. Rapid Commun.* **2005**, *26*, 1428–1433.
(57) Charoensirisomboon, P.; Inoue, T.; Weber, M. *Polymer* **2000**, *41*, 6907–6912.
(58) Pan, L.; Chiba, T.; Inoue, T. *Polymer* **2001**, *42*, 8825–8831.
(59) Pan, L.; Inoue, T.; Hayami, H.; Nishikawa, S. *Polymer* **2002**, *43*, 337–343.
(60) Maraschin, N. In *Encyclopedia of Polymer Science and Technology*, 3rd ed.; Mark, H. F., Ed.; John Wiley & Sons: New York, 2002; Vol. *2*, pp 412−441.
(61) Simpson, D. M.; Vaughan, G. A. In *Encyclopedia of Polymer Science and Technology*, 3rd ed.; Mark, H. F., Ed.; John Wiley & Sons: New York, 2002; Vol. *2*, pp 441−482.
(62) Jabbarzadeh, A.; Atkinson, J. D.; Tanner, R. I. *Macromolecules* **2003**, *36*, 5020–5031.
(63) Bhadane, P. A.; Virgilio, N.; Favis, B. D.; Champagne, M. F.; Huneault, M. A.; Tofan, F. *AIChE J.* **2006**, *52*, 3411–3420.
(64) Tsou, A. H., Qian, K. Unpublished data.

MA801390S